

Reliability Evaluation of Embeddable Reference Electrodes for Use in Reinforced Cement Concrete by Using TiO_2 Doped with SnO_2

Manjula N¹, Fowziya SA², Ayeshamariam A^{1,3*}, Selvan G^{1,4}, Thirumamagal R^{1,5}, Mohideen AMU² and Jayachandran M⁶

¹Research and Development Center, Bharathiyar University, Coimbatore, India

²Department of Chemistry, Khadir Mohideen College, Adirampattinam, India

³Department of Physics, Khadir Mohideen College, Adirampattinam, India

⁴Department of Physics, Thanthai Hans Rover College, Perambalur, India

⁵Department of Physics, Annada College, Devakottai, India

⁶Department of Physics, Sethu Institute of Technology, Pullor, Kariapatti, India

Abstract

Titanium dioxide represents an effective sensors and also used for the self-cleaning surfaces. Additionally, it can be used as antibacterial agent because of strong oxidation activity and super-hydrophilicity. Visible light-activated TiO_2 doped with SnO_2 could be prepared by RF sputtering, nonmetal doping or sensitizing of TiO_2 doped with SnO_2 . This paper reviews preparation methods of TiO_2 doped with SnO_2 with metallic and nonmetallic species, including various types of dopants and doping methods currently available. A further development along this line inductive resistance, other mass loss measurements for a sensing element in a corrosive environment.

Keywords: Cement; Electrodes; Concrete sensor; TiO_2 - SnO_2

Introduction

The importance of reference electrodes is undisputed practically in all electrochemical analytical methods. Particularly, the results rendered by potentiometry are all highly dependent on quality performance of the reference electrodes; thus, the actual development of novel electrodes selective to ions goes hand in hand with studies oriented to optimization of the former [1]. Apart from all the classical features that reference electrode should have, namely, to provide a constant potential that is stable with respect to the indicator electrode, that it should not be polarizable, it should return quickly to the correct imposed potential after an accidental polarization, its behavior should follow the Nernst Law for the pertinent species depending on the sort of electrode, that the potential be independent of the solution's composition and that the solid compound of the electrode have small solubility in the electrolyte [2]. Presently, it is required also that these electrodes are amenable to miniaturization and that they may be readily adapted to varied configuration as demanded by the analytical system.

It is well known that the most common reference electrodes are based on calomel, on sulphates and on Ag/AgCl, where the latter clearly exhibit superior characteristics regarding the miniaturization possibilities [3]. However, the conventional Ag/AgCl electrodes exhibit an important limitation concerning the internal solution and cannot comply with the aforementioned new characteristics required for the electrodes. Therefore, some interesting features have been developed to deal with this problem, such as miniaturization of the compartment containing the solution [4-7] and the use of polymers instead of water to immobilize the chloride ions [8-12]. Furthermore, the infrastructure to build these electrodes requires the use of high technology, which in the majority of cases turns out to be economically prohibitive. Therefore, several efforts have been made to develop the so called solid state Ag/AgCl reference electrodes, which eliminate the need of an internal chloride solution. The apparently simple fact of solution elimination from reference electrodes largely abates the complexity of their building techniques, which has led various researchers to develop and optimize diverse configuration for this sort of electrodes. Amidst one of the first reports published in this respect, that of Pungor et al. focused on the development of a reference electrode based on the coating of a silver wire with a $Ag-AgCl-(NH_4)_2CO_3$ mix held in

epoxy resin. The recent trend concerns the application of thick-film technology to build solid state reference electrode [13-16]. This kind of electrodes have been commercially exploited for a large variety of applications, using for their constructions commercially available dyes composed of a Ag/AgCl/polymer mix [17]. Aside the aforementioned strategy, others have also been occasionally used, like the use of polymeric membranes such as aromatic polyurethanes [18,19] and Nafion [20] to protect the Ag/AgCl layer of the electrode and to diminish possible ionic interference on its potential. The construction techniques recurrently reported in the literature indicate that flat configurations are commonly adopted for these electrodes, which at the same is interpreted as their current configurational restriction. This work present a novel construction strategy [21] of an Ag/AgCl reference electrode based on a composite containing a mixture of silver, AgCl, graphite and non conducting epoxy resin. Given characteristics of the composite reference electrodes (CRE) several configurations of the solid state electrode may be readily achieved and compared to conventional techniques previously described for the construction of the same that should be more accessible from an economic point of view.

Currently available probes do not meet all needs. A number of new innovative, inexpensive probes for monitoring the existing structures are therefore being developed, covering the most important deterioration mechanisms: corrosion of reinforcement, carbonation of concrete, freeze-thaw damage, alkali aggregate reaction and mechanical damage (over loading). The progress of these mechanisms can be predicted

***Corresponding author:** Ayeshamariam A, Research and Development Center, Bharathiyar University, Coimbatore and Department of Physics, Khadir Mohideen College, Adirampattinam, India, E-mail: aamariam786@gmail.com

Received February 15, 2018; **Accepted** February 22, 2018; **Published** March 05, 2018

Citation: Manjula N, Fowziya SA, Ayeshamariam A, Selvan G, Thirumamagal R, et al. (2018) Reliability Evaluation of Embeddable Reference Electrodes for Use in Reinforced Cement Concrete by Using TiO_2 Doped with SnO_2 . J Powder Metall Min 7: 186. doi:[10.4172/2168-9806.1000186](https://doi.org/10.4172/2168-9806.1000186)

Copyright: © 2018 Manjula N, et al. This is an open-access article distributed under the terms of the Creative Commons Attribution License, which permits unrestricted use, distribution, and reproduction in any medium, provided the original author and source are credited.

by monitoring key material parameters (temperature, moisture, pH, chloride concentration, corrosion current/rate/initiation), either on the surface or as a profile through the concrete in structure, as well as mechanical parameters (strain, deflection, vibration, acoustics) [22].

Calomel electrodes and other mercury-mercurous electrodes are formed from mercury and hence any leakage may lead to pollution hazard. Further use of aqueous solutions either potassium chloride or other salts require careful maintenance as well as careful handling. The process of making silver-silver halide electrodes is quite tedious as it involves either electro deposition or thermal decomposition. It is rather difficult to achieve stability, sensitivity, and reproducibility. The process of making metal-metal oxide electrode is also laborious as it involves using powdered metal-powered oxide in admixture [23].

Efforts have been ongoing for decades to monitor structural corrosion and environmental corrosivity. Many types of sensors have been used in a variety of applications in order to better understand and track parameters related to corrosion events. Such parameters include pH, temperature, humidity, oxygen levels, ionic concentrations (atmospheric or fluid chemistry), corrosion potential, corrosion current, electrochemical impedance, electrochemical noise, and others. The type of sensor measurements selected depends on the structure of interest, the environment in which it exists, and the expected forms of corrosion to which it might succumb. Sensors and multi-sensor units have found military and commercial monitoring applications in a wide variety of settings including, but not limited to, vehicles (e.g. ships, aircraft), infrastructure (e.g. bridges, tunnels), utilities (e.g. water, electricity), and industry (e.g. chemical processing, oil and gas production) [24].

Sensors can be divided into two main categories: those that determine corrosivity of the environment in contact with the structure of interest, and those that directly measure corrosion of the structure itself. In the first case, sensors return valuable information about the corrosivity of the local environment, either by measuring parameters that indirectly relate to corrosion phenomena, or by measuring self-corrosion of an element within the sensor unit itself. Sensors of these types may be used to monitor the environment of structures in immersion in natural or industrial waters, buried underground, embedded in concrete, exposed to atmosphere, or exposed to specialized industrial environments. In the second case, information about the actual condition and corrosion behavior of a structure, such as corrosion potential, coating condition, or loss of wall thickness, can be obtained. Certain corrosion sensors technologies and combined sensor units have the capability of monitoring both the structure and its environment. The list is not intended to be exhaustive but rather to provide a brief overview of developments in sensor and monitoring technology [25].

A variety of sensors have been developed to monitor environmental characteristics known to affect corrosion. Such characteristics can be including temperature, relative humidity, oxygen levels, dissolved or atmospheric ionic contamination and pH. Although there have been many methods over the years to monitor these types of system characteristics, improvements are still being made. The use of new "smart" materials such as advanced ceramics, composites, and polymers., for example, have led to successful improvements in monitoring of a number of corrosivity parameters in the oil and gas industry. Research has shown that the direct monitoring of moisture intrusion into coatings or hidden and hard-to-inspect locations on vehicles or structures can be performed by embedded coated fiber optic sensors with "smart" coating whose optical properties change

upon absorption of moisture. The benefits of improved and accurate monitoring of parameters such as cooling water pH, and hydrogen and oxygen content of high temperature water and steam are evident in the electrical power generation industry as well [26].

An environmental factor of concern in the natural gas industry is hydrogen availability in steel sour gas service pipelines. External factors that influence hydrogen-induced cracking (HIC) include temperature, pH and carbon dioxide and hydrogen sulfide partial pressures. Electrochemical sensors can be used to detect hydrogen in steel for comparison with the threshold concentration of hydrogen above which a steel is susceptible to HIC, and the pH of a corroding medium below which a steel is susceptible to HIC. Amperometric sensors measure equivalent flux of hydrogen through steel, from which the concentration of hydrogen at the inner pipe surface may be estimated. Potentiometric sensors allow determination of hydrogen equivalent pressure in the pipe steel, which can lead to concentration/activity estimates. Tests showed that both sensors were responsive to hydrogen in the steel tested, but the potentiometric sensors had greater sensitivity to the pH of the corrosive medium [27].

Much like corrosivity sensors, corrosion sensors have been developed to monitor the condition of ships and aircraft, pipelines and tanks, bridges and other infrastructure. Unlike corrosivity sensors that return information about an environment, corrosion sensors provide direct information about the condition of an actual structure. Intermittent or continuous monitoring of corrosion potential has long been a method for determining whether portions of a structure are passive, cathodically protected, or actively corroding. Reference electrodes are easily employed in environments such as soil, concrete, or any environment that has the capacity to act as an electrolyte in contact with the structure of interest (e.g. pipeline, rebar). Their on stability sometimes must be considered, however, especially in high temperature or varying temperature environments. Reference electrodes are useful for monitoring the corrosion potential of buried structures, especially if the ground has a moisture level sufficient to allow ionic current flow. Reference electrodes in combination with stainless steel resistivity probes were incorporated into a system to monitor a reinforced concrete transit tunnel. Electrically isolated sections 300 m in length were instrumented with embedded sensors. Reference electrodes for measuring potential of the rebar and stainless steel electrodes for current density measurements through the concrete were embedded at several points along each section. This allowed for successful remote DC stray current monitoring as well as monitoring of active/pассив conditions of the steel rebar.

For best results relative to a structure of interest, the sensor should be in as close to the same environment as possible and the sensing element should have corrosion behavior similar to that of the structure of interest. If the corroding elements of such sensors are made of the same or very similar materials as the structure of interest, this may improve the agreement between the corrosion rate measured by the sensor and the corrosion rate actually occurring at the structure. However, differences in manufacturing, handling, and even exposure time in the environment of interest may cause deviations between the corrosion rates of a sensing element and the structure it is intended to protect. These considerations are not critical, however, if the main concern is simply to obtain a general view of the corrosivity at a particular location.

An example of a corrosivity sensor that incorporates self-corroding elements is the bimetallic sensor. These atmospheric "time-of-wetness" sensors depend on a galvanic couple of two metals. Under conditions

of humidity conductive to condensation, an electrolyte layer is formed on the dissimilar metal surfaces, resulting in corrosion current. Atmospheric contaminants play a role by adding to the conductivity of the condensate layer. Elevated temperature may also play a role in the response of this type of sensor by accelerating corrosion of the galvanic couple. The resulting corrosion current is used to estimate corrosion conditions at the surface of the structure of interest, on or near which the sensor is mounted. One potential drawback of this type of sensing element is that the response of the galvanic couple may not be the same as that of the monitored structure in the same environment. Consequently, material selection for the sensor elements can play an important role in creating a unit that returns information that reflects the corrosion conditions of the structure of interest. In addition, devices that rely on self-corrosion, such as the bimetallic galvanic couple, of necessity have a limited life time since some portion of anode in the couple is consumed whenever the sensor is active [28].

Several other corrosivity sensors depend on a self-corroding element. Traditionally, these include electric resistance probes, linear polarization resistance, and electrochemical noise sensors. Electric resistance probes can be used in atmospheric, immersion, or underground service, and measure a change in electrical resistance between an electrode exposed to the environment and a nominally identical probe protected from that environment. Corrosion of the exposed element leads to a loss of cross section and a rise in electrical resistance. The resulting mass loss data are used to determine a general corrosion rate that in turn can be used to predict possible corrosion condition at the structure of interest. Electrical resistance probes operate on the same principle as traditional mass loss coupons exposed in a process stream, except that coupons must be removed and handled for mass loss evaluation where as resistance measurements may be made with the probe *in-situ*. Similar to electrical resistance probes, the inductive resistance probe has greater sensitivity to cross section change due to mass loss, and reduced sensitivity to temperature changes. As with the electrical resistance probe, corrosion rates for sensing element result [29].

Linear polarization resistance requires small DC perturbations (usually ± 30 mV around the open circuit corrosion potential) applied to an electrode in an immersion environment. As a result of these small perturbations a corrosion current proportional to the corrosion rate is measured. A three-electrode sensor system is used including the material of interest as the working electrode, a counter electrode to pass current through the electrolyte, and a reference electrode to monitor potential at the working electrode. A requirement for successful use of linear polarization resistance is a conductive electrolyte. Low conductivity solutions introduce substantial errors that lead to underestimates in corrosion rate. If the solution conductivity in the environment of interest is not high, other methods may be employed to compensate. For example, a probe that relies both on linear polarization resistance and galvanostatic current-interrupt method has been shown to compensate for the substantial IR drop seen in low conductivity solutions, leading to more realistic corrosion rate values.

Electrochemical noise measurements are performed with 2 or 3 electrode sensing elements. An example of potential use for the electrochemical noise technique is the monitoring of high-level nuclear waste storage tanks. Carbon steel double shell high-level waste storage tanks were monitored for a stress corrosion cracking and for pitting using a multi-electrode system designed to track both current and potential electrochemical noise. 3 nominally identical electrodes made up the sensing elements. The designating working and

counter electrodes (WE, CE respectively) were connected through a zero-resistance ammeter for measurements of instantaneous current fluctuation. The third, the pseudo-reference electrode (RE), was used to measure instantaneous potential fluctuations between the RE itself and the WE/CE pair. While the prototype consisted of the 3 sensing elements only, a more advanced version consisted of a set of eight 3-element sensors, stationed at various depths in the waste liquid as well as in the vapour phase space above the liquid waste. Consequently, corrosion rate and localized corrosion information could be obtained from the many different environments present within the enclosed space. An increased understanding of the localized corrosion contribution to the electrochemical noise signal is possible when the current and potential fluctuation data is analyzed in the frequency domain [30].

Experimental Section

Ordinary Portland cement was sieved through 150 μ m sieve and extracts was prepared as follows. To a 100 g of the cement added 100 ml of distilled water and shaken vigorously using a Microid flask mechanical shaker for about 1 hour. The extracts were then collected by filtration. AR grade CaO was heated for a long time to remove any carbonate present in the sample. About 1.85 g of CaO is dissolved in distilled water to get a saturated calcium hydroxide solution. Synthetic concrete pore solution consists of 7.4 g NaOH and 36.6 g KOH per liter of saturated calcium hydroxide solution. The experimental work in the present work deals with substrate cleaning, formation of pellet, which is the target for deposition and TiO_2 ; SnO_2 thin film deposition onto quartz substrates under appropriate conditions. These are explained below. An ultrasonic cleaner is a cleaning device that uses ultrasound (usually from 15-400 kHz) to clean delicate items.

In an ultrasonic cleaner, the object to be cleaned is placed in a chamber containing a suitable ultrasound conducting fluid. In aqueous cleaners, the chemical added is a surfactant which breaks down the surface tension of the water base. An ultrasound generating transducer is built into the chamber, or may be lowered into the fluid. It is electronically activated to produce ultrasonic waves in the fluid. The main mechanism of cleaning action is by energy released from the creation and collapse of microscopic cavitation bubbles, which break up and lift off dirt and contaminants from the surface to be cleaned. The higher the frequency, the smaller the nodes between the cavitations points which allows for more precise cleaning. The bubbles created are so small that cleaning and removal of dirt is the main result. TiO_2 powder (GR-99.9%-Aldrich) was taken with respect to its molecular (90% TiO_2 +10% SnO_2) weight and grinded by adding polyvinyl alcohol (PVA) solution [1 g PVA+100 ml distilled water] and consolidated in the form of a pellet (Dimension- dia" 5 cm and thickness 4 mm) by applying a uniaxial force of 15 Ton for three minutes using a hydraulic press. Extreme care was taken to see that the pelletization of the sample was done under uniform condition. The pellet was first sintered in the furnace for about 5 hours at 1200°C to make the particles get bind together. The pellet was compressed to quite dimensions. This pellet was used as the target for the thin film depositions. Similarly TiO_2 ; SnO_2 pellet also prepared by pressing and sintering methods [31].

Thin films of TiO_2 doped with SnO_2 were prepared under high vacuum ($\sim 10^{-5}$ torr) setup on ultrasonically cleaned Quartz substrates using planar DC magnetron sputtering unit. The target to substrate distance was fixed as 6 cm. The vacuum chamber was cleaned perfectly, and the target and substrates are mounted in their respective holders. The mains were made ON. The Rotary Pump (RP) is made ON. Backing was done till the vacuum reads 0.01 mbar (1 mbar=0.76 torr) in GH1 mode. Then roughing was done till it reads 0.05 mbar in GH2 mode.

The Diffusion Pump (DP) was set ON and left for 45 minutes for the oil to get heated. Then high vacuum valve was opened and a high vacuum atmosphere was created in the system environment till it reaches 10^{-5} mbar. The alkalinites of the various solutions were measured using a digital pH meter (model pH-300, Roy Instrument). Initially the pH meter was calibrated using alkaline buffer solutions. 5 ml of the extract is pipetted out into a conical flask and one or two drops of phenolphthalein indicator is added, 0.02 N sulphuric acid is added until the pink color disappears. Then add one or two drops of 5% potassium chromate solution and it is titrated against standard silver nitrate solution taken in the burette. Reddish brown color is the end point. TiO_2 (Dimension: 1.0 cm diameter, 16.00 cm breadth, 40.03 cm length) and SnO_2 (2.75 cm diameter, 15.50 cm breadth and 38.00 cm length) were taken for this study. The initial weight of the specimen was taken using Mettler balance triplicate specimens were introduced into a PVC see-through cell containing 250 ml of the cement extracts, CPS and sat.Ca (OH)₂. The test solution was changed every week in order to avoid carbonation of the solution. The temperature was maintained constant throughout these experiments at $35 \pm 1^\circ\text{C}$. Weight losses were measured before and after immersion in test solutions at the end of exposure of 30 days. This test is carried out in order to understand the chemical stability of the film in test solution.

During the immersion of sensor electrodes in test solutions, the sensor specimens were taken out frequently and the surfaces were carefully examined with magnifying lens. After the end of the exposure period, the specimens were removed from the test solutions, washed with water and seen through a microscope to examine the integrity of the surface [32].

This method is also described as Tafel plot method or Evans's diagram method or logarithmic polarization method. This method involves measurement of corrosion rate of the system, by the measurement of the potential of the electrode for various applied current densities. A plot of E vs. Log I give a figure known as polarization diagram.

The intercept of anodic and cathodic Tafel lines provides the corrosion current and Tafel slopes give b_a and b_c . In actual practice, polarization curves are obtained from galvanostatic/potentiostatic or potentiodynamic methods. Potentiodynamic polarization studies were carried out using TiO_2 or SnO_2 sensor in OPC extracts, saturated calcium hydroxide solution and concrete pore solution. Polarization were performed to evaluate the corrosion kinetic parameters such as corrosion current (I_{corr}), corrosion potential (E_{corr}), cathodic Tafel slope (b_c) and anodic Tafel slope (b_a). The different test solutions were prepared using distilled water. The working electrode was ITO or SnO_2 a sensor. The polarization cell is a 3-electrode glass cell assembly. A rectangular platinum foil was used as the counter electrode. The area of the counter electrode is much larger than the area of the working electrode. This will exert a uniform potential field on the working electrode. Reference electrode used was SCE ($\text{Hg}/\text{Hg}_2\text{Cl}_2/\text{sat.KCl}$). A constant quantity of the test solution was taken in the polarization cell. The working, counter and reference electrodes were assembled and connections were made [33].

The test solution was continuously stirred using a magnetic stirrer to avoid the concentration polarization. Time intervals of 10-15 minutes were given for each of the system to attain a steady state and the OCP was noted. Both anodic and cathodic polarization curves were recorded potentiodynamically using ACM instrument, UK. This instrument itself is having provisions for programs to evaluate corrosion kinetic parameters such as I_{corr} , E_{corr} , b_a and b_c . The potentiodynamic condition

corresponds to a potential sweep rate of 60 mV/minute and potential ranges of -200 to 200 V from the OCP. All the experiments were carried out at constant temperature of $35 \pm 1^\circ\text{C}$. A similar procedure as above was adapted for cyclic polarization studies also. The potentiodynamic condition corresponds to the potential sweep rate of 6 mV/minute and potential ranges of -20 to +20 from the OCP. Here the experiment is run for 2 cycles. The difference in the shifting of potential from the first cycle and the second cycle was noted [34].

An electrochemical impedance measurement is an appropriate method for corrosion studies, particularly for corrosion rate determinations, mechanistic studies, passivation and passivity process and for investigation in inhibited systems. R_s represent solution resistance. R_t or R_i gives charge transfer resistance and C_{dl} represents the double layer capacitance. Using Stern-Geary equation, I_{corr} is obtained from R_t since,

$$I_{corr} = \left(\frac{b_x b_c}{2.303(b_x + b_c)} \right) \left[\frac{1}{R_t} \right] \quad (1)$$

Thus, the cell impedance "Z" consist of real (Z') and imaginary ($-Z''$) parts. A plot of Z' Vs. $-Z''$ for various frequencies is a semicircle. At high frequency, Z corresponds to R_s and at low frequency Z corresponds to $(R_s + R_t)$ and the difference between the two values gives R_t . The double layer capacitance (C_{dl}) can be calculated from the frequency ω at the top of the semicircle ($-Z''$ maximum) [34-36].

$$F(-Z'' \text{ max}) = \left(\frac{1}{2X C_{dl} X R_t} \right) F(-Z'' \text{ max}) = \left(\frac{1}{2 X C_{dl} X R_t} \right) \quad (2)$$

This is the only A.C. method used under the present investigations. The three-electrode cell assembly was used here also. For this TiO_2 doped with SnO_2 sensor was used as working electrode; saturated calomel electrode used as reference electrode and platinum electrode used as counter electrode. They were assembled and connections were made. A time interval of 10 to 15 minutes was given for the OCP to reach a steady value. The impedance measurements were carried out using ACM Instruments, corrosion monitoring field machine. The real part (Z') and imaginary part ($-Z''$) of the cell impedance were measured for various frequencies (30 KHZ to 0.01 Hz). Plots Z' vs. $-Z''$ were made. Impedance measurements were carried out for TiO_2 doped with SnO_2 sensor in OPC extracts, saturated calcium hydroxide solutions and concrete pore solutions [37].

Characterization technique

TiO_2 doped with SnO_2 thin film were deposited on quartz substrate kept at room temperature using 13.56 MHz radio frequency magnetron sputtering system with 99.99% titanium oxide doped tin oxide (SnO_2 10%) ceramic target. Argon atmosphere was only used without adding oxygen. The quartz substrates were scrupulously cleaned in freshly prepared hot chromic acid for 1 hour and thoroughly cleaned with distilled water followed by ultrasonic cleaning for 1 hour. It is usually observed that under the operating conditions, the substrate temperature reaches about 40°C only when the substrate was placed at larger distance above the target. Hence, sputtering was carried out by placing the substrate at about 8 cm above the target throughout the experiment. The base pressure inside the chamber was 10^{-6} Torr and the argon pressure was maintained at 5×10^{-3} Torr. The RF power was varied between 50 W and 350 W in steps of 50 W and the duration of film deposition was kept constant at 30 min. Film thickness was measured by the Stylus Profilometer (Mitutoyo) and was maintained at about 300 nm for all the deposited film. The optical transmittance spectra were recorded in the wavelength range 200-2500 nm using a

Hitatchi-330 UV-Vis-NIR spectrophotometer. X-ray diffraction (XRD) measurements were carried out with X'pert Pro PANalytical-3040 using $\text{CuK}\alpha$ radiation ($\lambda=1.5406 \text{ \AA}$) to study the crystallinity of the films.

Results and Discussion

XRD patterns of the Nano sized TiO_2 doped with SnO_2 are shown in Figure 1a. In addition, Figure 1 Full wide-angle XRD re-scaled patterns of the TiO_2 and SnO_2 samples, diffraction from Sn or SnO_2 phases (JCPDS 41-1445, P42/mnm) was observed, demonstrating the complete dissolution of Sn^{4+} cations to form $\text{Sn}-\text{O}-\text{Ti}$ bonding and/or the formation of very small SnO_2 clusters well-dispersed among anatase TiO_2 crystallites. Slight shift in (1 0 1) and (0 0 4) diffractions in SnO_2 samples toward smaller 2-theta values, the peak intensity decrease and the peak width broadening occurred when Sn was doped into the material (seen inter scaled patterns in Figure 1a, indicating an increase in the lattice parameter and the decrease in average grain size stemming from the increase in disorder with the substitution of Sn into TiO_2 lattice sites. The XRD results are consistent with a fore mentioned HR-TEM findings. Due to the difference in ionic radii ($\text{Sn}=69 \text{ pm}$, $\text{Ti}=53 \text{ pm}$, $\text{Sn}^{4+}=0.69 \text{\AA}$, $\text{Ti}^{4+}=0.605 \text{\AA}$) [38], a lattice mismatch during the partial substitution of Sn^{4+} for Ti^{4+} in the TiO_2 lattice occurred, leading to lattice distortion and the generation of edge dislocations. Nevertheless, in spite of the observation of few SnO_2 particles in HR-TEM in TiO_2 sample, the absence of Sn or SnO_2 diffractions in XRD can be attributed to its low concentration that is below the instrumental detection limitation.

The structure of anatase, which are larger than those of pristine TiO_2 , indicating the lattice expansion when SnO_2 dopants with larger ionic radius ($\text{Sn}^{4+}=0.69 \text{\AA}$, $\text{Ti}^{4+}=0.605 \text{\AA}$) [39] are introduced. The distribution of Ti, O, and Sn elements in TiO_2 doped with SnO_2 composite can be seen on the elemental mapping from both FE-SEM with EDAX analysis, where the relative location of each constituent may be explained as shown in Figure 2a and 2b.

Mechanistic aspects TiO_2 doped with SnO_2 thin film as sensor in concrete environments

The electrochemical stability of thin film electrodes in concrete environments was measured with respect to saturated calomel electrode.

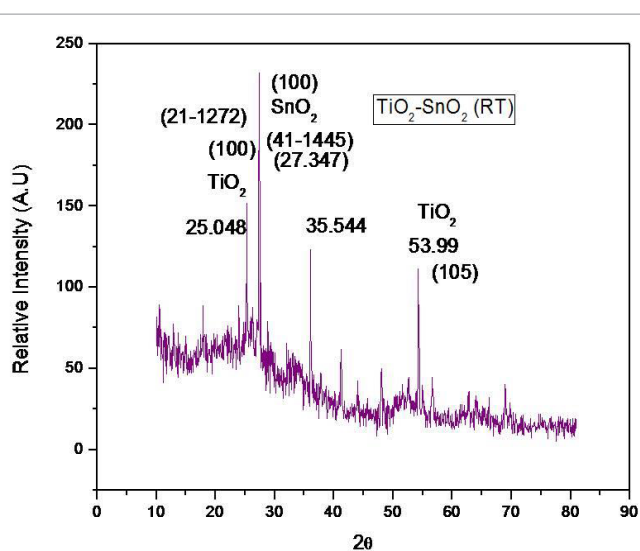


Figure 1: XRD analysis of TiO_2 - SnO_2 thin film.

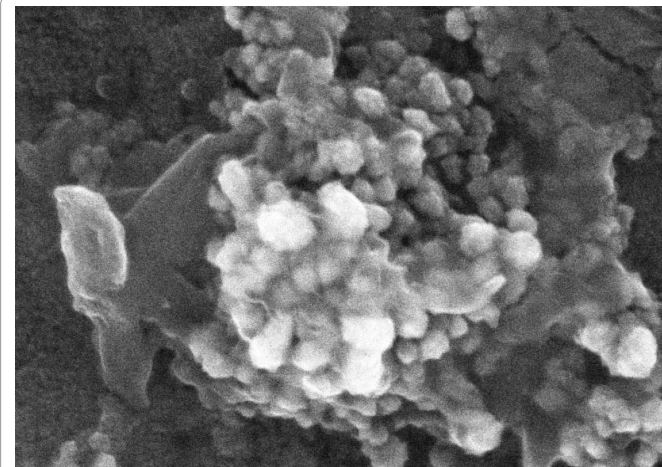


Figure 2: SEM analysis of TiO_2 doped with SnO_2 thin film at $\text{RT}^{\circ}\text{C}$.

The stability of the any sensor electrode is depends on the measure of the activity of the reactive species. If the activity of the species reacting at the sensing electrode varies, the potential also may vary. As first shown by Nernst, the electrode response may be described by a linear equation:

$$E = E_0 \pm S \log C \quad (3)$$

Where E =the measured voltage;

E_0 =a combination of several constants within the system including reference potentials;

S is the slope of the electrode;

C =activity of the measured species.

Most often it is desired to measure the concentration of species in a sample. At a fixed and constant ionic strength, activity is proportional to concentration. The Nernst equation may be rewritten to describe electrode response to the concentration (C) under these conditions:

$$E = E_0 \pm S \log a \quad (4)$$

So all the sensor electrodes are depends on how far they maintain the stability and the stability depends on the activity of the sensing element.

A good reference sensor must have to obey the two important pre-requisites:

- (i) Should be electrochemically stable (reliable potential readings) and
- (ii) Chemically stable (should not react with the environment).

In this aspect TiO_2 doped with SnO_2 film are found suitable sensor for embeddable use into the concrete structures. It is a well known fact that, a good embeddable electrode should have the ability to sustain small currents with less polarization and hysteresis effects. It should be stable, cost effective and should be able to fabricate using an environmentally safe manufacturing process. In this regard, TiO_2 doped with SnO_2 electrode provides a reliable embeddable sensor for corrosion monitoring of concrete structures. Hence, lot of scope will be there to utilize TiO_2 doped with SnO_2 film as possible alternative candidate materials as potential sensor for corrosion monitoring of reinforcing steel in concrete structures.

The stability of TiO_2 doped with SnO_2 film sensor electrode was tested in three concrete environments namely cement extract, concrete pore solution and Sat. $\text{Ca}(\text{OH})_2$ for the exposure period of 30 days. The surface of the film was examined daily and found that no significant changes in the surface. The film was intact and no surface delamination was noticed. The thin films after cycling in various alkaline solutions have been subjected to XRD studies.

The resistance of the coated side was measured using high impedance voltmeter. The resistance of the film was as same as the initial value. It indicates the chemical stability of the TiO_2 doped with SnO_2 film sensor was excellent in said concrete environments. Interestingly no weight loss was noticed at the end of the exposure period. No delamination of film was noticed in all the three concrete environments at the end of the exposure period. Materials Tin (IV) chloride fuming (Riedel-de Haën, SnCl_4) and titaniumn-butoxide (Aldrich, $\text{Ti}(-\text{OC}_4\text{H}_9)_4$) were used as TiO_2 and SnO_2 pre-cursors. All the chemicals reagents were used as purchased without further purification. In a typical procedure, a solution of SnCl_4 and anhydrous ethanol (40 mL) was stirred at room temperature, followed by the drop-wise addition of deionized water and HCl (37 wt%) [40].

The reversibility characteristics of the TiO_2 - SnO_2 at RT sensor in concrete environments were carried out by cyclic sweep method. Reversibility curve for TiO_2 - SnO_2 at RT film sensor in cement extract is shown in Figure 3. The corresponding reversibility parameters are given in Table 1. It is interesting to note that $E_{\text{corr}1}$ and $E_{\text{corr}2}$ for the TiO_2 - SnO_2 at RT C in cement extract are -180 mV and -185 mV vs. SCE

respectively. Similarly, the reversibility curve for TiO_2 - SnO_2 at RT°C film sensor in concrete pore solution is shown in Figures 4 and 5 reversibility parameters are given in Table 2. The $E_{\text{corr}1}$ for the TiO_2 doped with SnO_2 in concrete pore solution was found to be -190 mV and $E_{\text{corr}2}$ was -195 mV. As observed earlier, here again the difference between $E_{\text{corr}1}$ and $E_{\text{corr}2}$ for the TiO_2 - SnO_2 at RT film sensor in sat. $\text{Ca}(\text{OH})_2$ is 5 mV .

It was interesting to note that the average potential difference between first cyclic curve and second cyclic curve was 5 mV in the said concrete environments.

System	$E_{\text{corr}1}$ mV vs. SCE	$E_{\text{corr}2}$ mV vs. SCE	Difference $E_{\text{corr}1}$ & $E_{\text{corr}2}$ mV vs. SCE
CE	-180	-185	5
CPS	-190	-195	5
Sat.CaO	-190	-195	5
Average			5

Table 1: Reversibility parameters for TiO_2 doped with SnO_2 film in concrete environments.

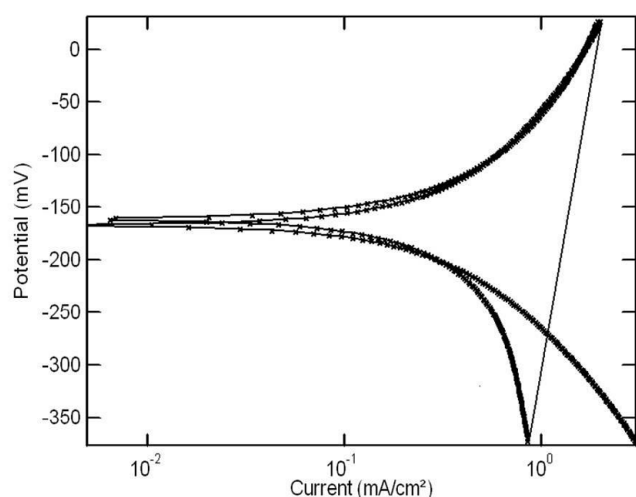


Figure 4: Polarization curve for TiO_2 doped with SnO_2 film sensor in cement extract.

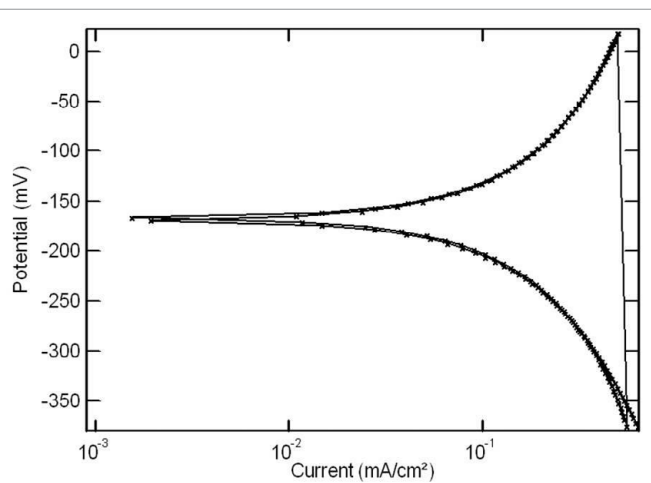


Figure 3: Polarization curve for TiO_2 doped with SnO_2 thin film at RT°C.

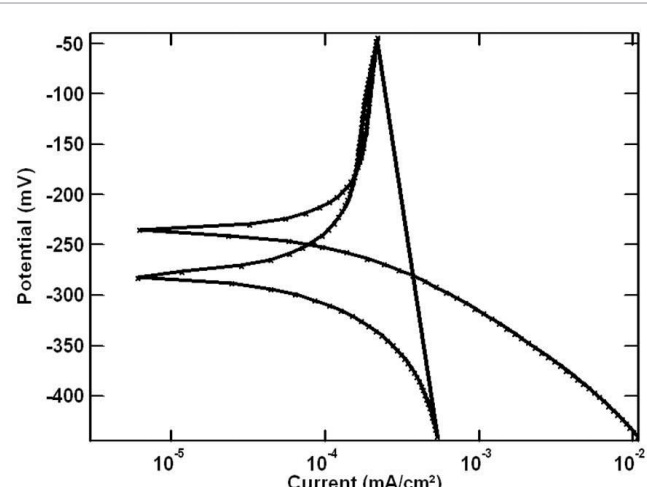


Figure 5: Polarization curve for TiO_2 doped with SnO_2 film sensor in sat $\text{ca}(\text{OH})_2$.

System studied	OCP mv Vs SCE	b_a mV.dec ⁻¹	b_c mV.dec ⁻¹	I_{corr} mA.cm ⁻²
CE	-301	102	73	0.0020
CPS	-304	100	72	0.0081
Sat CaO	-300	111	73	0.0025
Average				0.0042

Table 2: Polarization parameters for TiO_2 doped with SnO_2 thin film in concrete environments film sensor in sat ca ($\text{OH})_2$.

The following important observation was made on a TiO_2 doped with SnO_2 sensor in that solution:

Average OCP=-304 mV vs. SCE

Average charge transfer resistance= $3.8913 \times 10^5 \Omega.\text{cm}^2$

Average double layer capacitance= $6.314 \times 10^{-5} \text{ F}$

The R_{ct} values are almost same in three test solutions. This is to observe both TiO_2 doped with SnO_2 thin film in concrete environments. This behavior indicates the perfect uniformity of TiO_2 doped with SnO_2 thin films in three test solutions. Uniformity is the important criteria to assemble any sensor for any purpose or use. In this mean, TiO_2 doped with SnO_2 definitely show a good uniformity in concrete environments.

Conclusion

TiO_2 doped with SnO_2 thin film was prepared by RF Sputtering technique and characterized by using X-ray diffractometer to find the crystal structure and its size of 77 nm and to find the morphological studies of SEM analysis was observed, with reference to the electrodes concrete sensor was analyzed and reported. Cyclic voltammetry method clearly explained the current density and its ability to sense the materials.

References

1. Suzuki H, Shiroishi H, Sasaki S, Karube I (1999) Microfabricated liquid junction Ag/AgCl reference electrode and its application to a one-chip potentiometric sensor. Analytical Chemistry 71: 5069-5075.
2. Caton Jr RD (1973) Reference electrodes. Journal of Chemical Education 50: A571.
3. Suzuki H, Hirakawa T, Sasaki S, Karube I (1998) Micromachined liquid-junction Ag/AgCl reference electrode. Sensors and Actuators B: Chemical 46: 146-154.
4. Ito S, Kobayashi F, Baba K, Asano Y, Wada H (1996) Development of long-term stable reference electrode with fluoric resin liquid junction. Talanta 43: 135-142.
5. Van Den Berg A, Grisel A, Van Den Vlekkert HH, De Rooij NF (1990) A micro-volume open liquid-junction reference electrode for pH-ISFETs. Sensors and Actuators B: Chemical 1: 425-432.
6. Nolan MA, Tan SH, Kounaves SP (1997) Fabrication and characterization of a solid state reference electrode for electro-analysis of natural waters with ultra-microelectrodes. Analytical Chemistry 69: 1244-1247.
7. Mroz A (1998) Disposable reference electrode. Analyst 123: 1373-1376.
8. Lindner E, Buck RP (2000) Micro-fabricated potentiometric electrodes and their in vivo applications.
9. Bakker E (1999) Hydrophobic membranes as liquid junction-free reference electrodes. Electro-analysis 11: 788-792.
10. Suzuki H, Hiratsuka A, Sasaki S, Karube I (1998) Problems associated with the thin-film Ag/AgCl reference electrode and a novel structure with improved durability. Sensors and Actuators B: Chemical 46: 104-113.
11. Lee HJ, Hong US, Lee DK, Shin JH, Nam H, et al. (1998) Solvent-processible polymer membrane-based liquid junction-free reference electrode. Analytical Chemistry 70: 3377-3383.
12. Ciobanu M, Wilburn JP, Buss NI, Ditavong P, Lowy DA (2002) Miniaturized reference electrodes based on Ag/AgI internal reference elements. I. manufacturing and performance. Electro analysis 14: 989-997.
13. Schnakenberg U, Liseic T, Hintsche R, Kuna I, Uhlig A, et al. (1996) Novel potentiometric silicon sensor for medical devices. Sensors and Actuators B: Chemical 34: 476-480.
14. Desmond D, Lane B, Alderman J, Glennon JD, Diamond D, et al. (1997) Evaluation of miniaturized solid state reference electrodes on a silicon based component. Sensors and Actuators B: Chemical 44: 389-396.
15. Eine K, Kjelstrup S, Nagy K, Syverud K (1997) Towards a solid state reference electrode. Sensors and Actuators B: Chemical 44: 381-388.
16. Simonis A, Krings T, Lüth H, Wang J, Schöning MJ (2001) A hybrid thin-film pH sensor with integrated thick-film reference. Sensors 1: 183-192.
17. Koopal CGJ, Bos AACM, Nolte RJM (1994) Third-generation glucose biosensor incorporated in a conducting printing ink. Sensors and Actuators B: Chemical 18: 166-170.
18. Yoon HJ, Shin JH, Lee SD, Nam H, Cha GS, et al. (2000) Solid-state ion sensors with a liquid junction-free polymer membrane-based reference electrode for blood analysis. Sensors and Actuators B: Chemical 64: 8-14.
19. Lee JS, Lee SD, Cui G, Lee HJ, Shin JH, et al. (1999) Hydrophilic polyurethane coated silver/silver chloride electrode for the determination of chloride in blood. Electro analysis 11: 260-267.
20. Moussy F, Harrison DJ (1994) Prevention of the rapid degradation of subcutaneously implanted Ag/AgCl reference electrodes using polymer coatings. Analytical Chemistry 66: 674-679.
21. Álvarez-Romero GA, Morales-Pérez A, Rojas-Hernández A, Palomar-Pardavé M, Ramírez-Silva MT (2004) Development of a Tubular Sensor Based on a Polypyrrole-Doped Membrane for the Potentiometric Determination of the Dodecylsulfate Anion in a FIA System. Electro analysis 16: 1236-1243.
22. Moody GJ, Oke RB, Thomas JDR (1970) A calcium-sensitive electrode based on a liquid ion exchanger in a poly (vinyl chloride) matrix. Analyst 95: 910-918.
23. Alegret S, Alonso J, Bartroli J, Paulis JM, Lima JLFC, et al. (1984) Flow-through tubular PVC matrix membrane electrode without inner reference solution for flow injection analysis. Analytica Chimica Acta 164: 147-152.
24. Muralidharan S, Saraswathy V, Thangavel K, Palaniswamy N (2008) Electrochemical studies on the performance characteristics of alkaline solid embeddable sensor for concrete environments. Sensors and Actuators B: Chemical 130: 864-870.
25. Manning DG, Schell HC (1985) Early Performance of Eight Experimental Cathodic Protection Systems at the Burlington Bay Skyway Test Site.
26. Muralidharan S, Saraswathy V, Madhavamayandi A, Thangavel K, Palaniswamy N (2008) Evaluation of embeddable potential sensor for corrosion monitoring in concrete structures. Electrochimica Acta 53: 7248-7254.
27. Gurusamy KN, Geoghegan MP (1990) The long term performance of embedded reference electrodes for cathodic protection and in situ monitoring of steel in concrete. Corrosion of Reinforcement in Concrete, pp: 333-347.
28. Anwar MS, Sujitha B, Vedalakshmi R (2014) Light-weight cementitious conductive anode for impressed current cathodic protection of steel reinforced concrete application. Construction and Building Materials 71: 167-180.
29. Spis RCA, Huchtemann P (1986) Prevention of Mild Steel Dissolution in Sulphuric Acid by Glutaraldehyde. Glutaraldehyde has been found as an excellent inhibitor for mild steel dissolution in sulphuric acid. Performance of glutaraldehyde. Thyssen Edelstahl Tech Eer 12: 190-195.
30. Liu Y, Weyers RE (1998) Modeling the time-to-corrosion cracking in chloride contaminated reinforced concrete structures. Materials Journal 95: 675-680.
31. Jones DA (1992) Principles and prevention of corrosion. Macmillan.
32. Arup H, Klinghoffer O, Mietz J (1997) Long term performance of MnO₂-reference electrodes in concrete. In Corrosion97. NACE International.
33. Ayeshamariam A, Kashif M, Bououdina M, Hashim U, Jayachandran M, et al. (2014) Morphological, structural, and gas-sensing characterization of tin-doped indium oxide nanoparticles. Ceramics International 40: 1321-1328.
34. Yeau KY, Kim EK (2005) An experimental study on corrosion resistance of concrete with ground granulate blast-furnace slag. Cement and Concrete Research 35: 1391-1399.

35. Liu ZL, Cui ZL, Zhang ZK (2005) The structural defects and UV-VIS spectral characterization of TiO₂ particles doped in the lattice with Cr³⁺ cations. Materials Characterization 54: 123-129.
36. Štengl V, Bakardjieva S, Murafa N (2009) Preparation and photo-catalytic activity of rare earth doped TiO₂ nanoparticles. Materials Chemistry and Physics 114: 217-226.
37. Tuinstra F, Koenig JL (1970) Raman spectrum of graphite. The Journal of Chemical Physics 53: 1126-1130.
38. Kelly S, Pollak FH, Tomkiewicz M (1997) Raman spectroscopy as a morphological probe for TiO₂ aerogels. The Journal of Physical Chemistry B 101: 2730-2734.
39. Noguchi S, Sakata H (1980) Electrical properties of undoped In₂O₃ films prepared by reactive evaporation. Journal of Physics D: Applied Physics 13: 1129.
40. Wickersham CE, Greene JE (1978) The effect of substrate bias on the electrical and optical properties of In₂O₃ films grown by RF sputtering. Physica Status Solidi 47: 329-337.